Polyhedron 102 (2015) 344–352

Contents lists available at ScienceDirect

Polyhedron

journal homepage: www.elsevier.com/locate/poly

Multinuclear NMR and crystallographic study of diorganotin valproates – Part II

B.P. de Morais [a], G.M. de Lima [a,*], C.B. Pinheiro [b], R.A. Burrow [c], D.F. Back [c], R.A.S. San Gil [d], D.C. Menezes [e], José D. Ardisson [f]

[a] Departamento de Química, Universidade Federal de Minas Gerais, UFMG, Avenida Antônio Carlos 6627, Belo Horizonte, MG CEP 31270-901, Brazil
[b] Departamento de Física, Universidade Federal de Minas Gerais, UFMG, Avenida Antônio Carlos 6627, Belo Horizonte, MG CEP 31270-901, Brazil
[c] Departamento Química, Universidade Federal Santa Maria, BR-97115900 Santa Maria, RS, Brazil
[d] Instituto de Química, Universidade Federal do Rio de Janeiro, UFRJ, Avenida Athos da Silveira Ramos, 149, Cidade Universitária RJ, CEP 21941-909, Brazil
[e] Departamento de Química, Universidade Federal de Viçosa, UFV, Avenida Peter Henry Rolfs s/n, Viçosa, MG CEP 36570-001, Brazil
[f] Centro de Desenvolvimento em Tecnologia Nuclear, CDTN/CNEN, Avenida Antônio Carlos 6627, Belo Horizonte MG CEP 31270-901, Brazil

ARTICLE INFO

Article history:
Received 24 August 2015
Accepted 2 October 2015
Available online 9 October 2015

Keywords:
Organotin carboxylate
Stannoxanes
Solid state NMR
Structural determination
Drum-like organotin structure

ABSTRACT

The reactions of SnR_2Cl_2 {R = Me, Bu and Ph} and sodium valproate, $NaO_2CCH(CH_2CH_2CH_3)_2$, NaOVp yielded three diorganotin valproates $[\{(Me_2SnOVp)_2O\}_2]$ (**1**), $[\{(Bu_2SnOVp)_2O\}_2]$ (**2**) and $[\{PhSn(O)OVp\}_6]$ (**3**). These stannoxanes have been authenticated in terms of infrared, ^1H and ^{13}C NMR, and solution- and solid-state ^{119}Sn NMR and ^{119}Sn Mössbauer spectroscopy. In addition the crystallographic structures of complexes (**1**)–(**3**) have been determined by X-ray diffraction. Complexes (**1**) and (**2**) displayed two major signals in the ^{119}Sn NMR spectra in solution corresponding to the exo and endocyclic SnR_2 moiety of the stannoxanes. Other minor resonances have been also observed due to dynamic processes in solution. However in the ^{119}Sn MAS-NMR experiments only two down field signals were detected for complex (**1**), according to the presence of the exo and endocyclic organotin fragments, but with different resonance in comparison with the chemical shift obtained in solution. On the other hand little difference was observed in the ^{119}Sn chemical shift of complex (**3**) since only one resonance was detected in solution- or in the solid-state experiments, and the signals are very close to each other.

1. Introduction

Although tributyltin oxide (TBTO), due to its biocide efficiency has been used as anti-fouling paints, [1,2] it has been banned in several nations in view of serious environmental problems [3,4]. Even though organotin derivatives rank as some of the most widely used organometallic compounds [5,6] and other potential applications still surprise the experts in the field of medicinal inorganic chemistry [7–9]. Many works have described the preparation and characterization of organotin carboxylates [10–12] and noteworthy are their performance against tumours, fungi, bacteria, and other microorganisms [1,13–16].

Nowadays, resistance of microorganisms and toxicity are some of the major problems concerning the clinical use of drugs. Metal-based clinic treatments could provide alternative and attractive therapeutic routes to overcome this challenge. Therefore the search for new metal-containing antimicrobial drugs, more bio-specific and less toxic to the host and to the environment is of particular urgency. In spite of the intense investigation of the biological activity of organotin(IV) compounds, a complete understanding of their mode of action has yet to be established. However, a general pattern has emerged. The activities of organotin (IV) compounds are dependent on both the covalently bonded organic groups and the nature of the ligands [17]. Tri-substituted alkyl and aryltin(IV) compounds are generally more toxic than di-substituted organotin(IV) compounds, while mono-substituted are still less toxic [18]. However, the order of toxicity depends on the microorganism, and varies from strain to strain [19]. Inhibitory activity increases in the order Et < ^{n}Bu < Ph, that assists the crossing of the microorganism membrane, connecting toxicity of the organotins with their hydrophobicity and lipophilicity [17,20,21]. Besides preparing new organotin-dithiocarbamates, investigating their potential applications [22] and screening their activity in the presence of some parasites [23] we have been interested in the mechanism of action of such complexes in biological media [24,25]. The effect of organotin-dithiocarbamate and -carboxylate complexes on the cellular activity of some variety of

* Corresponding author. Tel.: +55 31 3409 5744; fax: +55 31 3409 5720.
E-mail address: gmlima@ufmg.br (G.M. de Lima).

http://dx.doi.org/10.1016/j.poly.2015.10.001
0277-5387/

Candida albicans revealed no changes in DNA integrity or in the mitochondria function of the cells. However, all complexes reduced the ergosterol biosynthesis affecting the membrane integrity. Special techniques used for morphological investigations such as scanning electron microscopy (SEM) and transmission electron microscopy (TEM) suggested that the organotin complexes act on the cell membrane, in view of the observed cytoplasm leakage and strong deterioration of the cellular membrane.

Valproic acid (VOpH) finds its major use in the treatment of some mental disorder, vastly documented in the literature, however its potential application as antitumoral drug has been discovered recently [26] and its synergic effect with organotin fragments has been investigated [27]. In a recent paper we have described the structural characterization of triorganotin valproates in terms of X-ray crystallography and NMR in solution and in the solid state. We have also described the biocide activity of the complexes towards some fungi [28]. In this paper we provide an NMR study, in solution and in the solid state, correlating the results with those obtained from X-ray crystallography and other spectroscopic techniques.

2. Experimental

2.1. Chemistry

2.1.1. Materials and instruments

All starting materials were purchased from Aldrich, Alfa Aesar, Fluka, Merck, Vetec or Synth and used as received. NMR spectra in solution were recorded at 200 MHz using a Bruker DPX-200 spectrometer equipped with an 89 mm wide-bore magnet. NMR spectra in solid state were recorded at 400 MHz using a Bruker Advance III DPX-400 spectrometer equipped with an 89 mm wide-bore magnet. ^{1}H and ^{13}C{^{1}H} shifts are reported relative to $SiMe_4$ and ^{119}Sn shifts relative to $SnMe_4$. The infrared spectra were recorded with samples pressed as KBr pellets on a Perkin–Elmer 238 FT-IR spectrometer in the range of 4000–400 cm^{-1}. Carbon, hydrogen and nitrogen analysis were performed on a Perkin–Elmer PE-2400 CHN-analysis using tin sample-tubes. Tin analysis were performed on a Hitachi Z-8200 spectrometer. ^{119}Sn Mössbauer spectra were run in standard equipment at liquid nitrogen temperature using a $BaSnO_3$ source kept at room temperature. Intensity data for the X-ray study were collected at 270(2) and 120(2) K on a Xcalibur, Atlas, Gemini, Kα/Mo (λ = 0.7107 Å). Data collection, reduction and cell refinement were performed using the CrysAlis RED program [29]. The structures were solved and refined employing the SHELXS-97 [30]. Further details are given in Table 3. All non-H atoms were refined anisotropic. The H atoms were refined with fixed individual displacement parameters [Uiso (H)Z1.2 Ueq (C)] using the SHELXL riding model. The ORTEP-3 program for windows [31] was used in the preparation of Figs. 1–3, sketched employing the Mercury program [32].

2.2. Syntheses

2.2.1. Synthesis of [{(Me$_2$SnOVp)$_2$O}$_2$] (**1**)

To a round bottom flask (250 mL) charged with NaOVap (1.00 g, 6.02 mmol) in EtOH (100 mL) was added $SnMe_2Cl_2$ (0.67 g, 3.05 mmol) dissolved in 20 mL of EtOH. After 5 h of reflux the reaction vessel was left to settle down, and NaCl was removed by filtration. The solvent was pumped off and the remaining white solid was recrystallized in a mixture of CH_2Cl_2/MeOH/H_2O (10:10:1) yielding X-ray quality crystals of (**1**). Yield 81%. Mp 165–167 °C. IR (cm^{-1}): 1614, 1566 (ν_{as} CO_2^-), 1418, 1396 (ν_s CO_2^-), 492 (ν Sn–O). ^{1}H NMR (δ, $CDCl_3$): 2.28 {m, $O_2CCH(CH_2CH_2CH_3)_2$}, 1.52–1.19 {m, $O_2CCH(CH_2CH_2CH_3)_2$}, 0.89 {$^{3}J_{(^{1}H4\text{-}^{1}H5)}$ = 6.6 Hz} {t, $O_2CCH(CH_2CH_2CH_3)_2$}, 0.76 {$^{2}J_{(^{119}Sn\text{-}^{1}H)}$ = 87.1 Hz} {s, $Sn(CH_3)_3$}; ^{13}C NMR (δ, $CDCl_3$): 183.2 {$O_2CCH(CH_2CH_2CH_3)_2$}, 47.2 {$O_2CCH(CH_2CH_2CH_3)_2$}, 35.4 {$O_2CCH(CH_2CH_2CH_3)_2$}, 21.1 {$O_2CCH(CH_2CH_2CH_3)_2$}, 14.4 {$O_2CCH(CH_2CH_2CH_3)_2$}, 9 and 7.3 {$Sn(CH_3)_2$}. ^{119}Sn NMR (δ, $CDCl_3$) −186.4 (very weak), −176.3 (strong) {$^{1}J_{(^{119}Sn\text{-}^{13}C)}$ = 773 Hz} {$^{2}J_{(^{119}Sn\text{-}^{117}Sn)}$ = 98.6 Hz} and −127.4 (very weak). ^{119}Sn MAS-NMR (δ_{iso}, 13 kHz): −202.0 and −239.7. ^{119}Sn Mössbauer δ (mm s^{-1}) 1.19; Δ (mm s^{-1}) 3.48. Elemental analysis for $C_{40}H_{84}O_{10}Sn_4$ (MW 1199.82 g mol^{-1}) found(calc): C, 40.18 (40.04); H, 7.14 (7.06); Sn, 39.06 (38.63).

2.2.2. Synthesis of [{(Bu$_2$SnOVp)$_2$O}$_2$] (**2**)

Prepared in a similar manner using NaOVp, (1.00 g 6.02 mmol) and $SnBu_2Cl_2$ (0.94 g, 3.09 mmol). X-ray quality crystals of (**2**) were obtained in the same mixture of solvent. Yield 69%. Mp 144.7–147.0 °C. IR (cm^{-1}): 1626, 1556 m (ν_{as} CO_2^-), 1416, 1396 m (ν_s CO_2^-), 473 (ν Sn–O). ^{1}H NMR (δ, $CDCl_3$): 2.19 {m $O_2CCH(CH_2CH_2CH_3)_2$}, 1.62–1.36 {$O_2CCH(CH_2CH_2CH_3)_2$}, 0.90 {$^{3}J_{(^{1}H4\text{-}^{1}H5)}$ = 7.0 Hz} {t, $O_2CCH(CH_2CH_2CH_3)_2$}, 1.62–1.36 {m, $Sn(CH_2CH_2CH_2CH_3)_3$}, 0.90 {t, $Sn(CH_2CH_2CH_2CH_3)_3$}; ^{13}C NMR (δ, $CDCl_3$): 182.9 {$O_2CCH(CH_2CH_2CH_3)_2$}, 47.5 {$O_2CCH(CH_2CH_2CH_3)_2$}, 35.4 {$O_2CCH(CH_2CH_2CH_3)_2$}, 21.2 {$O_2CCH(CH_2CH_2CH_3)_2$}, 14.4 {$O_2CCH(CH_2CH_2CH_3)_2$}, 27.9–26.7, {$Sn(CH_2CH_2CH_2CH_3)_3$}, 13.7 {$Sn(CH_2CH_2CH_2CH_3)_3$}. ^{119}Sn NMR (δ, $CDCl_3$) −214.0 {$^{2}J_{(^{119}Sn\text{-}^{117}Sn)}$ = 116 Hz}; −207.3 {$^{2}J_{(^{119}Sn\text{-}^{117}Sn)}$ = 112 Hz}; −182.7 (very weak) and −153.4 (weak). ^{119}Sn Mössbauer δ (mm s^{-1}) 1.31, Δ (mm s^{-1}) 3.42. Elemental analysis for $C_{64}H_{132}O_{10}Sn_4$ (MW 1536.45 g mol^{-1}) found(calc): C, 50.19 (50.02); H, 8.86 (8.66); Sn, 30.90 (30.14).

2.2.3. Synthesis of [{PhSn(O)OVp}$_6$] (**3**)

Similarly prepared using $SnPh_2Cl_2$ (1.07 g, 3.11 mmol) and sodium valproate, NaOVp (1.00 g, 6.02 mmol). After washing with hot water the oily product was recrystallized in a mixture of CH_2Cl_2/MeOH (1:1) from which suitable crystals for X-ray experiments were obtained. Yield 72%. Mp 330 °C(d). IR (cm^{-1}): 1590 (ν_{as} CO_2^-); 1427 (ν_s CO_2^-); 438 (ν Sn–O). ^{1}H NMR (δ, $CDCl_3$): 7.53–6.85 {m, $Sn(C_6H_5)_3$}; 2.37 {m, $O_2CCH(CH_2CH_2CH_3)_2$}, 1.60–1.36 {m, $O_2CCH(CH_2CH_2CH_3)_2$}, 0.87 {t, $O_2CCH(CH_2CH_2CH_3)_2$}; ^{13}C NMR (δ, $CDCl_3$): 185.4 {$O_2CCH(CH_2CH_2CH_3)_2$} 48.3 {$O_2CCH(CH_2CH_2CH_3)_2$}; 35.2 {$O_2CCH(CH_2CH_2CH_3)_2$}; 21.3 {$O_2CCH(CH_2CH_2CH_3)_2$}; 14.4 {$O_2CCH(CH_2CH_2CH_3)_2$}; 144.2 {C_α, $Sn(C_6H_5)_3$}; 135.5 {$^{2}J_{(^{119}Sn\text{-}^{13}C)}$ = 69.7 Hz}{C_β, $Sn(C_6H_5)_3$}; 127.7 {$Sn(C_6H_5)_3$}; 130.2 {C_γ, $Sn(C_6H_5)_3$}; {$^{4}J_{(^{119}Sn\text{-}^{13}C)}$ = 25.4 Hz}128.8 {C_δ, $Sn(C_6H_5)_3$}. ^{119}Sn NMR (δ, $CDCl_3$): −542.9. ^{119}Sn MAS-NMR (δ_{iso}, 13 kHz): −542.0; ^{119}Sn Mössbauer δ (mm s^{-1}): 0.62; Δ (mm s^{-1}): 1.87. Elemental analysis for $C_{84}H_{120}O_{18}Sn_6$ (MW = 2129.91 g mol^{-1}): found(calc): C, 48.16 (47.37); H, 5.62 (5.68); Sn, 33.44 (33.46).

3. Results and discussions

3.1. Chemistry

The complexes [{(Me$_2$SnOVp)$_2$O}$_2$] (**1**), [{(Bu$_2$SnOVp)$_2$O}$_2$] (**2**) and [{PhSn(O)OVp}$_6$] (**3**) were obtained according to Scheme 1, following the reactions of NaOVp with $SnMe_2Cl_2$, $SnBu_2Cl_2$ or $SnPh_2Cl_2$ in ethanol. The two first reactions rendered $R_2Sn(OVp)_2$ {R = Me and Bu} as primary products which were isolated and characterized by infrared and ^{1}H, ^{13}C, solution-state ^{119}Sn-NMR and melting points. The stannoxanes were produced during the process of re-crystallization effected by hydrolysis in ethanol. They have been isolated as colourless and crystalline solids and their purity were attested in terms of the satisfactory melting points and by C, H and Sn elemental analysis. The melting points (mp) of the intermediates $R_2Sn(OVp)_2$ {R = Me and Bu}, and of the corresponding stannoxanes are quite different. The melting point

Table 1
NMR data for complexes (**1**)–(**3**).

Attribution	$[\{(Me_2SnOVp)_2O\}_2]$ (**1**)	$Me_2Sn(OVp)_2$	$[\{(Bu_2SnOVp)_2O\}_2]$ (**2**)	$Bu_2Sn(OVp)_2$	$[\{PhSn(O)OVp\}_6]$ (**3**)
H2	2.28 (m, 1H)	2.44 (m, 1H)	2.19 (m, 1H)	2.44 (m, 1H)	2.37 (m, 1H)
H3, H3′	1.52–1.19 (m, 8H)	1.67–1.16 (m, 8H)	1.62–1.36 (m, 24H)	1.77–1.23 (m, 14H)	1.60–1.36 (m, 8H)
H4, H4′	1.52–1.19 (m, 8H)	1.67–1.16 (m, 8H)	1.62–1.36 (m, 24H)	1.77–1.23 (m, 14H)	1.60–1.36 (m, 8H)
H5, H5′	0.89 (t, 12H) {^3J = 6.6 Hz}	0.90 (t, 9H) {^3J = 7.0 Hz}	0.90 (t, 15H)	0.89 (t, 9H) {^3J = 7.0 Hz}	0.87 (t, 6H)
Hα	0.76 (s, 12H) {^2J = 87.1 Hz}	0.96 (s, 9H) {^2J = 80.5 Hz}	1.62–1.36 (m, 24H)	1.77–1.23 (m, 14H)	–
Hβ, Hβ′	–	–	1.62–1.36 (m, 24H)	1.77–1.23 (m, 14H)	7.53–6.85 (m, 5H)
Hγ, Hγ′	–	–	1.62–1.36 (m, 24H)	1.77–1.23 (m, 14H)	7.53–6.85 (m, 5H)
Hδ	–	–	0.90 (t, 15H)	0.89 (t, 9H) {^3J = 7.0 Hz}	7.53–6.85 (m, 5H)
C1	183.2	187.3	182.9	187.4	185.4 {^2J = 32.9 Hz}
C2	47.2	45.3	47.5	45.4	48.3
C3	35.4	35.0	35.4	35.0	35.2/34.7
C4	21.1	21.0	21.2	21.0	21.3/20.7
C5	14.4	14.2	14.4	14.2	14.4/14.2
Cα	9.0/ 7.3	4.9	27.0/26.7	25.4 {^1J = 594/569 Hz}	144.2
Cβ, Cβ′	–	–	27.9/27.6	27.0	135.5 {^2J = 69.7 Hz}
Cγ, Cγ′	–	–	27.3/27.2	26.6 {^3J = 97.3 Hz}	127.7
Cδ	–	–	13.7	13.7	128.8 {^4J = 25.4 Hz}

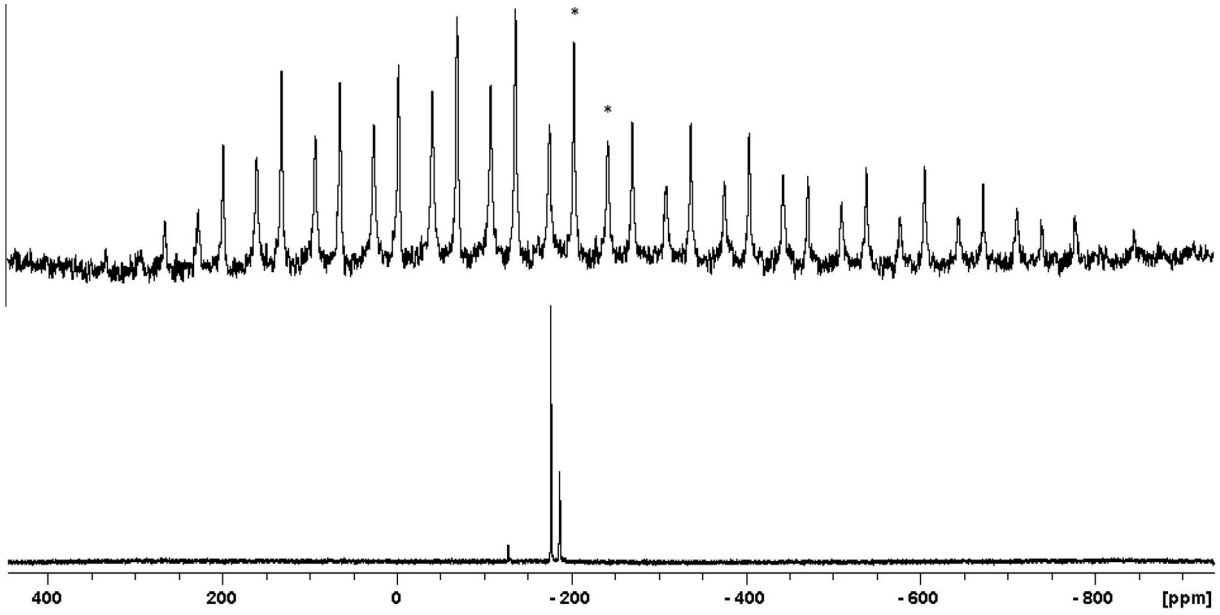

Fig. 1. Solid- and solution-state ^{119}Sn NMR spectra of $[\{(Me_2SnOVp)_2O\}_2]$ (**1**).

of (**1**) was found at 165–167 °C and its intermediate $Me_2Sn(OVp)_2$ melts in the range of 99–100 °C. The melting point of (**2**) ranged in the interval of 145–147 °C and for $Bu_2Sn(OVp)_2$ it was 86–88 °C, and complex (**3**) decomposes at 330 °C. Complex (**3**) was formed straight from the reaction of $SnPh_2Cl_2$ with NaOVp in ethanol and the corresponding stannoxane was not detected. The cleavage of the Sn–Ph bond in the presence of strong acids has been reported in the literature and widely used in chemical reactions involving organotin fragments [33,34]. However it is the first time that such bond breaking is produced by a metallic carboxylate.

3.2. Infrared results

A number of work points out in the literature the importance of the $\Delta\nu_{COO^-}$ (ν_{as}–ν_s) in the study of the Sn-carboxyl coordination [35–37]. In this paper the Na(OVp) displayed the following signals in the infrared spectrum (ir), $\Delta\nu_{COO^-}$ at 138 cm^{-1} (ν_{as} = 1554 cm^{-1}; ν_s = 1416 cm^{-1}). The vibration patterns of (**1**) and (**2**) are comparable with the signals displayed by the intermediates, $R_2Sn(OVp)_2$. Moreover these experiments could not reveal differences of the terminal and bridging valproate groups in the stannoxanes. Only one stretching frequency assigned to the carboxylate group was observed in the infrared spectra of (**1**)–(**3**) [ν_{as} = 1568 cm^{-1}, ν_s = 1412 cm^{-1} (**1**); ν_{as} = 1568 cm^{-1}, ν_s = 1398 cm^{-1} (**2**); ν_{as} = 1590 cm^{-1}, ν_s = 1427 cm^{-1} (**3**)]. Therefore, the following values of $\Delta\nu_{COO^-}$ were found 156, 170 cm^{-1} and 163 cm^{-1}, for (**1**)–(**3**) respectively, [38] corroborating to the presence of bridging carboxylates, as confirmed by the X-ray crystallographic experiments. It was also detected the presence of strong Sn–O bands in the region of 630–438 cm^{-1}.

3.3. NMR results

Experiments of ^{1}H, ^{13}C and ^{119}Sn NMR were performed with the stannoxanes (**1**)–(**3**), as well as with the intermediates of complexes (**1**) and (**2**), {$Me_2Sn(OVp)_2$ and $Bu_2Sn(OVp)_2$}, revealing chemical and magnetic differences, Scheme 2.

In view of the hydrogen resonances obtained in ^{1}H NMR experiments, only one type of valproate group or R moiety was observed in the intermediates $Me_2Sn(OVp)_2$ and $Bu_2Sn(OVp)_2$. On the other

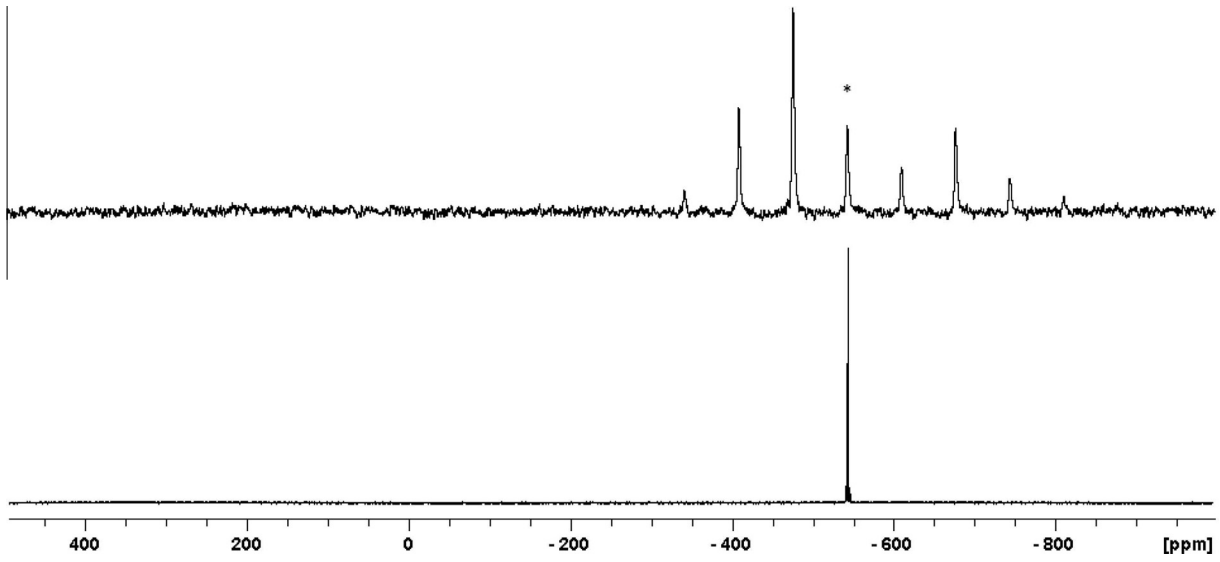

Fig. 2. Solid- and solution-state ^{119}Sn NMR spectra of [{PhSn(O)OVp}$_6$] (**3**).

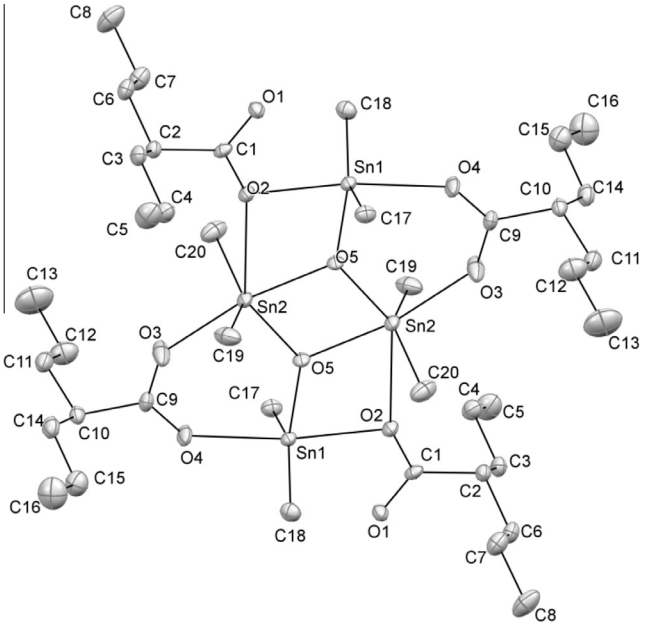

Fig. 3. The molecular structure of [{(Me$_2$SnOVp)$_2$O}$_2$] (**1**).

hand two different valproate fragments are observed in complexes (**1**) and (**2**), attributed to the endo and exocyclic organotin fragment, where the H atoms in the valproate are numbered as H3, H3′, H4, H4′ and H5, H5′, Table 1. Duplicated signals of ^{1}H were not detected in the region of the Me or Bu groups. Another interesting feature concerns the H$^{\alpha}$ of Me or Bu group that are more shielded in stannoxanes (**1**) and (**2**) than in the intermediates Me$_2$Sn(OVp)$_2$ and Bu$_2$Sn(OVp)$_2$. In addition the $^2J_{(^{119}Sn-^1H)}$ in (**1**), 87 Hz is bigger than in the intermediate Me$_2$Sn(OVp)$_2$, 80.5 Hz.

Despite the presence of three different valproate and Ph groups in (**3**), revealed by the X-ray crystallographic determination, the differences in the hydrogen resonances were not observed in ^{1}H NMR experiments, Table 1. It is possible that the free rotation of these organic groups might average the signals.

The main interest in the ^{13}C NMR spectra in this work concerns the resonances of the R groups and those of the carboxylate moiety, as well as the ^{119}Sn–^{13}C coupling constants. These experiments revealed significant differences between the spectra of the intermediates and those of the stannoxanes (**1**) and (**2**). Only one valproate group and SnR$_2$ fragment were observed in the spectra of the intermediates, Me$_2$Sn(OVp)$_2$ and Bu$_2$Sn(OVp)$_2$. For the butyl derivative the following ^{119}Sn–^{13}C couplings were observed: $^1J_{(^{119/117}Sn-^{13}C\alpha)}$ = 594/569 Hz and $^3J_{(^{119}Sn-^{13}C\beta)}$ = 97.3 Hz. Upon hydrolysis the chemical shift patterns of complexes (**1**) and (**2**) changed, mainly in terms of the SnR$_2$ fragments, exhibiting two signals for each carbon of the R moiety. No changes were observed in the carbon resonances of the valproate ligand despite the existence of bridging and terminal groups in (**1**) and (**2**). The ^{119}Sn–^{13}C couplings were not detected in the ^{13}C NMR spectra of (**1**) and (**2**), Table 1.

For complex (**3**), the ^{13}C NMR experiments in solution revealed subtle differences in the valproate groups which were not detected in the X-ray crystallographic experiments. It was observed a pair of resonance, C$_3$, C$_3'$, C$_4$, C$_4'$ and C$_5$, C$_5'$, as if the two carbon arms of the valproate group are no longer magnetically equivalent. Only one signal was displayed for C$_2$ and for the –CO_2^- fragment. In addition, it was observed an unusual coupling between the ^{119}Sn and ^{13}C of the –CO_2^- fragment, $^2J_{(^{119}Sn-^{13}C)}$ = 32.9 Hz. No magnetic differences were detected for the carbon atoms of the Ph ring, and only the second order coupling constant, ^{119}Sn–^{13}C$_\beta$ = 69.7 Hz was observed, Table 1.

The ^{119}Sn NMR spectrum of Me$_2$Sn(OVp)$_2$ and Bu$_2$Sn(OVp)$_2$ in solution, Fig. 1, revealed single signals at δ −127.2 and at −152.7, respectively. The stannoxanes [{(Me$_2$SnOVp)$_2$O}$_2$] (**1**) and [{(Bu$_2$SnOVp)$_2$O}$_2$] (**2**) displayed a more intricate ^{119}Sn chemical shift patterns. For complex (**1**) it was observed 3 signals δ −127.4 (very small), −176.3{main signal, $^1J_{(^{119}Sn-^{13}C)}$ = 596 Hz and $^2J_{(^{117}Sn-^{119}Sn)}$ = 96 Hz) and −186.4 (main signal). The two main signals are attributed to the exo and endocyclic organotin fragment present in the stannoxane and the signal at δ −127.4 is assigned to the presence of a tiny amount of the intermediate, Me$_2$Sn(OVp)$_2$, not entirely hydrolysed. Complex (**2**) exhibited two main signals at δ −207.0 {$^1J_{(^{119}Sn-^{13}C)}$ = 112 Hz} and -214 {$^1J_{(^{119}Sn-^{13}C)}$ = 116 Hz} corresponding to the exo and endocyclic fragment, and two other minor signals at δ −152.8, corresponding to the intermediate Bu$_2$Sn(OVp)$_2$, and at δ −182.7 possibly associated to a dynamic process in solution, Fig. 2. Possible doubts about the purity of complexes (**1**) and (**2**) might be disregarded in view of the sharp melting points and elemental analysis. The solid state

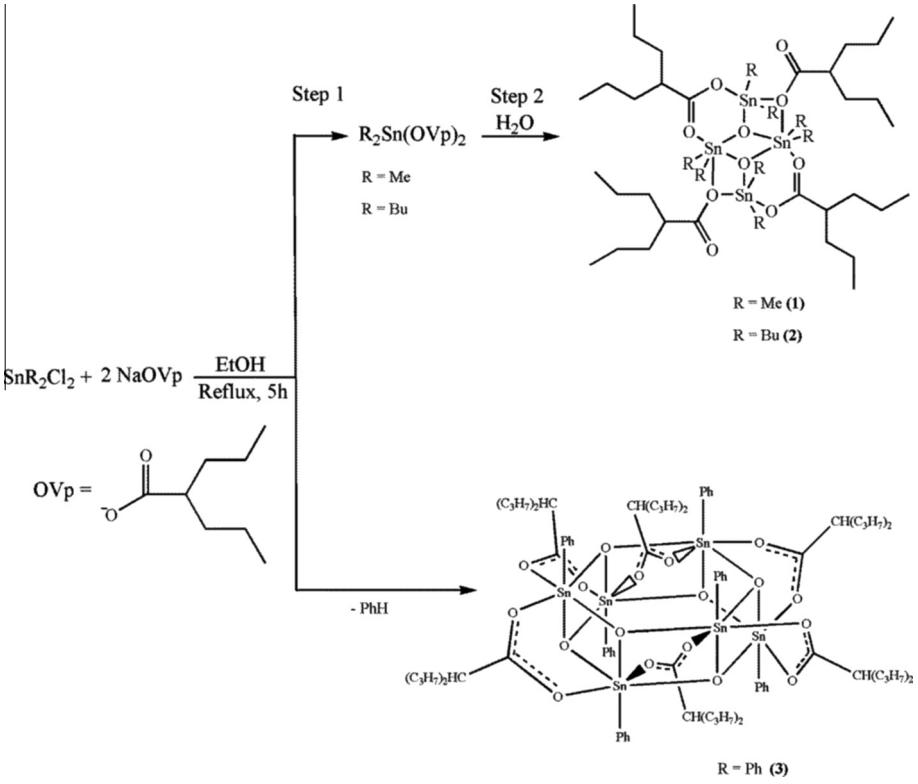

Scheme 1. Synthetic details of the preparation of complexes (**1**)–(**3**).

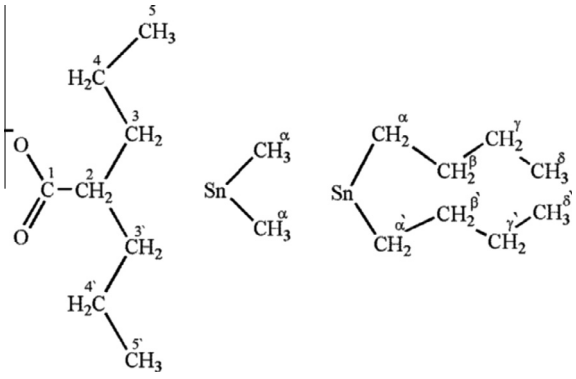

Scheme 2. Atom numbering for the NMR chemical shifts assignments.

^{119}Sn MAS-NMR experiments revealed two ^{119}Sn chemical shift assigned to the exo and endocyclic organotin fragment, δ_{iso} −202.5 (10 kHz) and −241.4 (10 kHz), for complex (**1**). The small difference between δ and δ_{iso} for (**1**) can be associated to solvation that weakens the intermolecular associations in the solid. On the other hand little difference was observed in the ^{119}Sn chemical shift of complex (**3**) at δ −542.9 and δ_{iso} −541.9, suggesting that this structure remains unchanged in solution.

The ^{119}Sn MAS NMR experiments did not show the $J_{(^{119}Sn-^{13}C)}$ coupling constants of complexes (**1**)–(**3**).

3.4. ^{119}Sn-Mössbauer spectroscopic results

The structure and the corresponding ^{119}Sn parameters of the organotin precursors used in this work are as follows: [$SnMe_2Cl_2$] {distorted tetrahedral, δ = 1.54 mm s^{-1} and Δ = 3.55 mm s^{-1}}, [39]; [$SnBu_2Cl_2$] {δ = 1.63 mm s^{-1} and Δ = 3.45 mm s^{-1}} [40]; [$SnPh_2Cl_2$] {tetrahedral, δ = 1.48 mm s^{-1} and Δ = 2.80 mm s^{-1}}, [41]. Upon complexation we have observed the following parameters for complexes (**1**)–(**3**), [{($Me_2SnOVp)_2O$}$_2$] (**1**), δ = 1.19 mm s^{-1} and Δ = 3.48 mm s^{-1}; [{($Bu_2SnOVp)_2O$}$_2$] (**2**) δ = 1.31 mm s^{-1} and Δ = 3.42 mm s^{-1}; [{PhSn(O)OVp}$_6$] (**3**), δ = 0.62 mm s^{-1} and Δ = 1.87 mm s^{-1}. Despite the presence of the endo and exocyclic $SnMe_2$ fragment, which are chemically and magnetically different, their geometric arrangements are similar. Therefore the ^{119}Sn Mössbauer spectroscopic experiments were not sensitive enough to display such restrained structural variations. The X-ray crystallographic determination of (**1**) revealed that the chemical surroundings at the Sn atom changes from a distorted tetrahedral to a slightly distorted trigonal bipyramid. The decrease in the isomer shift from 1.54 mm s^{-1} in $SnMe_2Cl_2$ to 1.19 mm s^{-1} in (**1**) is a consequence of the re-hybridization from sp^3 to sp^{3}d, revealing a decrease in *s* contribution to the frontiers molecular orbitals. The same tendency is observed for complex (**2**), since δ varies from 1.63 mm s^{-1} in $SnBu_2Cl_2$ to 1.31 mm s^{-1} in (**2**) because of the same re-arrangement of orbitals. The coordination process of $SnPh_2Cl_2$ with the valproate ligand changes the tin environment in the organotin halide, from tetrahedral to octahedral. So, that explains the reason of the strong decrease of the s orbitals contribution in complex (**3**), since the isomer shift changes from 1.48 to 0.62 mm s^{-1}. The symmetry of charge in complex (**1**) and (**2**) differs a little from the starting organotin halides as revealed by the small variation in the quadrupolar splitting. However the Δ of complex (**3**), 1.87 mm s^{-1}, is quite different from that described in the literature for $SnPh_2Cl_2$, 2.80 mm s^{-1}, showing a more symmetric chemical environment at the tin atom in complex (**3**).

3.5. X-ray crystallographic results

Crystallographic authentication of new therapeutically active substances turns to be important, since the delicate structural

Table 2
The crystallographic parameters of structural determination of complexes (**1**)–(**3**).

Compound	(**1**)	(**2**)	(**3**)
Empirical formula	$C_{40}H_{84}O_{10}Sn_4$	$C_{64}H_{132}O_{10}Sn_4$	$C_{84}H_{120}O_{18}Sn_6$
Formula weight	1199.83	1536.45	2129.94
T (K)	270	100	110
λ (Å)	0.71073	0.71073	0.71073
Radiation	Mo Kα	Mo Kα	Mo Kα
Crystal system	triclinic	triclinic	monoclinic
Space group	$P\bar{1}$	$P\bar{1}$	$P1\ 21/n1$
a (Å)	11.5586 (3)	11.7382(10)	13.2923(4)
b (Å)	11.5895 (3)	12.6927(10)	19.4168(5)
c (Å)	11.6925 (3)	14.1103(10)	18.3320(6)
α (°)	65.655 (3)	63.573 (3)	90
β (°)	72.595 (2)	77.021 (3)	107.957(3)
γ (°)	72.128 (2)	87.047 (3)	90
V (Å^3)	1330.99 (6)	1831.7 (3)	4500.9(2)
Z	1	1	2
Calculated density (Mg m^{-3})	1.497	1.393	1.572
μ (mm^{-1})	1.90	1.40	1.701
F(000)	604	796	2136
Crystal size (mm)	0.23 × 0.14 × 0.07	0.37 × 0.14 × 0.13	0.43 × 0.18 × 0.13
θ (°)	2.35–30.51	4.5–20.7	2.3–27.5
T_{min}, T_{max}	0.848, 0.949	0.748, 0.840	0.612, 0.822
Limiting indices	$h = -16 \rightarrow 16$	$h = -14 \rightarrow 14$	$h = -16 \rightarrow 17$
	$k = -16 \rightarrow 16$	$k = -14 \rightarrow 15$	$k = -25 \rightarrow 25$
	$l = -16 \rightarrow 16$	$l = -17 \rightarrow 17$	$l = -23 \rightarrow 23$
Reflections collected	41 116	49 901	57 958
Independent reflections (R_{int})	8137 (0.051)	6886 (0.056)	10 282 (0.07)
Reflections obs.	5564	4337	7606
Absorption correction	analytical	analytical	analytical
Refinement method	full-matrix least-squares on F^2	full-matrix least-squares on F^2	full-matrix least-squares on F^2
Data/restrains/parameters	8137/0/252	6886/0/473	10 282/0/470
Goodness-of-fit (GOF) on F^2	1.157	1.026	1.113
$R[F^2 > 2\sigma(F^2)]$	0.037	0.049	0.038
$wR(F^2)$	0.086	0.126	0.088
S	1.16	1.03	1.11
$\Delta\rho_{max}$	1.87 e Å^{-3}	1.23 e Å^{-3}	1.37 e Å^{-3}
$\Delta\rho_{min}$	−0.90 e Å^{-3}	−0.93 e Å^{-3}	−1.01 e Å^{-3}
$(\Delta/\sigma)_{max}$	0.001	<0.001	0.001

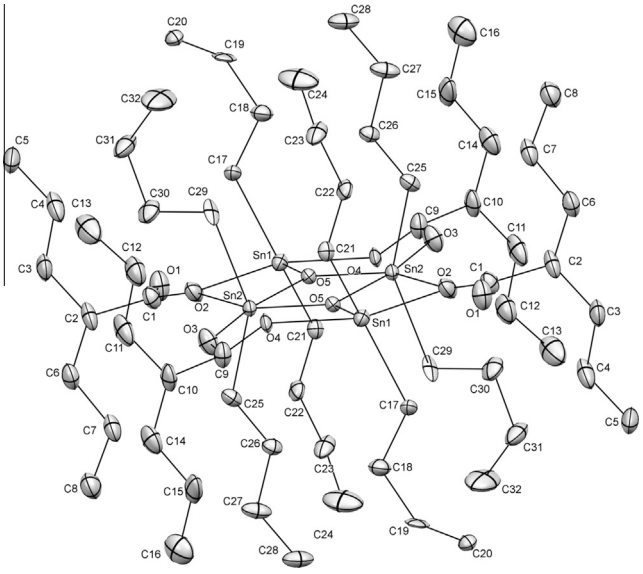

Fig. 4. The molecular structure of [{($Bu_2SnOVp)_2O}_2$] (**2**), view 1.

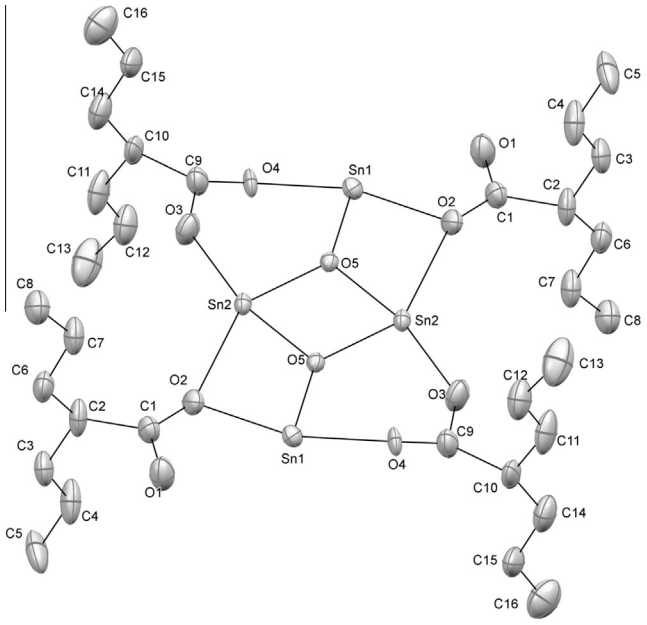

Fig. 5. The molecular structure of [{($Bu_2SnOVp)_2O}_2$] (**2**), view 2.

differences of molecules in solution- and in the solid-state play a key role to understand the biological interaction of drugs with cells or microorganisms and the corresponding mechanism. The literature reports that organotin carboxylates can adopt several crystallographic arrangements. It has been nicely reviewed in the last decade [42]. The structure of complexes (**1**)–(**3**) was determined by X-ray diffraction experiment, Table 2.

Complexes (**1**) and (**2**) display the known ladder type structure, however with mutually terminal and bridging carboxylates, which is less usual [40]. They crystallise in the triclinic system, space group $P\bar{1}$ and the X-ray crystallographic study, Figs. 3–5, revealed

Table 3
Selected bond length and angles of complexes (**1**) and (**3**).

Compound	Selected bond lengths (Å)		Selected angles (°)			
[{($Me_2SnOVp)_2O}_2$] **(1)**	Sn(1)-O(5)	2.050(2)	O(2)-Sn(1)-O(4)	170.8(1)		
	Sn(1)-O(2)	2.198(2)	O(5)-Sn(1)-C(17)	105.4(1)		
	Sn(1)-O(4)	2.254(3)	O(5)-Sn(1)-C(18)	105.4(1)		
	Sn(1)-C(17)	2.088(6)	C(17)-Sn(1)-C(18)	148.9(2)		
	Sn(1)-C(18)	2.092(5)	O(3)-Sn(2)-O(5)	167.6(1)		
	Sn(2)-O(5)	2.040(2)	O(5)-Sn(2)-C(19)	108.3(1)		
	Sn(2)-O(5′)	2.133(2)	O(2)-Sn(2)-C(19)	77.9(1)		
	Sn(2)-O(3)	2.229(3)	O(2)-Sn(1)-C(20)	78.5(1)		
	Sn(2)-C(20)	2.096(5)	O(5)-Sn(2)-C(20)	108.4(2)		
	Sn(2)-C(19)	2.095(6)				
[{($Bu_2SnOVp)_2O}_2$] **(2)**	Sn(1)-O(2)	2.231(6)	O(2)-Sn(1)-O(4)	164.4(3)		
	Sn(1)-O(4)	2.320(2)	O(5)-Sn(1)-C(17)	110.5(5)		
	Sn(1)-O(5)	2.043(5)	O(5)-Sn(1)-C(21)	109.4(4)		
	Sn(1)-C(17)	2.230(2)	C(17)-Sn(1)-C(21)	139.2(6)		
	Sn(1)-C(21)	2.052(2)	O(5)-Sn(2)-C(29)	102.7(7)		
	Sn(2)-O(5′)	2.043(4)	O(5)-Sn(2)-O(3)	102.7(7)		
	Sn(2)-O(5)	2.153(4)	O(5)-Sn(2)-C(29)	141.90(3)		
	Sn(2)-O(2)	2.791(6)	O(5)-Sn(2)-C(25)	110.2(2)		
	Sn(2)-O(3)	2.284(8)	C(25)-Sn(1)-C(29)	146.6(8)		
	Sn(2)-C(25)	2.108(6)				
	Sn(2)-C(29)	2.297(2)				
[{$PhSn(O)OVp\}_6$] **(3)**	Sn(1)-O(1)	2.093(3)	O(2)-Sn(1)-O(3)	102.6(1)	O(3)-Sn(2)-O(4)	87.1(1)
	Sn(1)-O(2)	2.084(3)	O(1)-Sn(1)-O(1)	78.4(1)	O(2′)-Sn(2)-O(5)	131.4(1)
	Sn(1)-O(3)	2.089(3)	O(3)-Sn(1)-O(1)	78.1(1)	O(1)-Sn(2)-O(5)	85.8(1)
	Sn(1)-O(6)	2.151 (3)	O(2)-Sn(1)-O(6)	158.2(1)	O(3)-Sn(2)-O(5)	88.9(1)
	Sn(1)-O(8)	2.164 (3)	O(3)-Sn(1)-O(6)	89.8(1)	O(4)-Sn(2)-O(5)	77.4(1)
	Sn(2)-O(1)	2.089(3)	O(1)-Sn(1)-O(6)	86.9(1)	O(3′)-Sn(3)-O(1)	104.5(1)
	Sn(2)-O(2′)	2.088(3)	O(2)-Sn(1)-O(8)	86.0(1)	O(3′)-Sn(3)-O(2)	77.9(1)
	Sn(2)-O(3)	2.093(3)	O(3)-Sn(1)-O(8)	162.8(1)	O(1)-Sn(3)-O(2)	78.2(1)
	Sn(2)-O(4)	2.147(3)	O(1)-Sn(1)-O(8)	89.3(1)	O(3′)-Sn(3)-O(9)	85.7(1)
	Sn(2)-O(5)	2.155(3)	O(6)-Sn(1)-O(8)	77.8(1)	O(1)-Sn(3)-O(9)	161.5(1)
	Sn(3)-O(1)	2.087(3)	O(2′)-Sn(2)-O(1)	103.3(1)	O(2)-Sn(3)-O(9)	89.2(1)
	Sn(3)-O(2)	2.100(3)	O(2′)-Sn(2)-O(3)	77.9(1)	O(3′)-Sn(3)-O(7)	157.8(1)
	Sn(3)-O(3′)	2.082(3)	O(1)-Sn(2)-O(3)	78.1(1)	O(3′)-Sn(3)-O(7)	88.5(1)
	Sn(3)-O(7)	2.150(3)	O(2′)-Sn(2)-O(4)	89.3(1)	O(2)-Sn(3)-O(7)	87.5(1)
	Sn(3)-O(9)	2.139(3)	O(1)-Sn(2)-O(4)	157.9(1)	O(9)-Sn(3)-O(7)	77.3(1)

that the centrosymmetric dimmers possesses an inversion centre located at the four-member Sn_2O_2 distorted ring.

There are two crystallographic distinct tin cations in the structure, Sn1 and Sn2 outlining the exo and endocyclic SnR_2 fragments. In both structures, the exocyclic tin cation (Sn1) lie at the centre of a distorted trigonal bipyramid, surrounded by two carbons at the equatorial position and three oxygens, two in the apical coordination and the other one located at the third equatorial corner. The exocyclic rings in (**1**) and (**2**) are formed by the following chemical distances: Sn(1)–O(2) = 2.198(2) Å, Sn(1)–O(4) = 2.254(3) Å (axial coordination), Sn(1)–O(5) = 2.050(2) Å, Sn(1)–C(17) = 2.088(6) Å and Sn(1)–C(18) = 2.092(5) Å (equatorial contacts), (1); Sn(1)–O(2) = 2.231(6) Å, Sn(1)–O(4) = 2.249(1) Å (axial coordination), Sn(1)–O(5) = 2.043(5) Å, Sn(1)–C(17) = 2.230(2) Å and Sn(1)–C(21) = 2.052(2) Å (equatorial contacts), (2). In (1) and (2) the longer Sn–O bonds, with O(2) and O(4), are from the coordination of valproate groups, monodentate and bidentate respectively, while the shorter contact involves an oxide anion, O(5). The exocyclic Sn–C in (1), Sn(1)–C(17) = 2.088(6) Å and Sn(1)–C(18) = 2.092(5) Å, are less asymmetric than in (2), Sn(1)–C(17) = 2.230(2) Å and Sn(1)–C(21) = 2.052(2) Å. The axial angles in (**1**) and (**2**), O5–Sn1–O3, 170.8(1)° and 167.4(3)°, respectively, are nearly related, however smaller than 180°. The mean values of the equatorial angles 119.9° and 119.7°, in (**1**) and (**2**) are close to 120°, the expected equatorial angles for a perfect trigonal bipyramid, Table 3.

The endocyclic Sn(2) cations in (**1**) and (**2**) are located at the centre of a distorted octahedral, sketched by the asymmetric coordination of bridging oxygens and the bonding to the carbon atoms of the organic groups [Me (**1**) and Bu (**2**)]. In complex (**1**) the axial bonds are: Sn(2)–O(5) = 2.132(3) Å and Sn(2)–O(3) = 2.225(4) Å and in (2) these bonds are 2.153(4) and 2.284(8) Å. The O(3)–Sn(2)–O(5) angles in (**1**) and (**2**), 167.6(1) and 166.0(2)°, respectively, are narrower than 180°, the expected angle of the axial position of an octahedral. The corners of the equatorial position in (**1**) are occupied by C(19), C(20), O(2) and O(5′) and in (**2**) by C(25), C(29), O(2) and O($\bar{5}$). The chemical bonds are Sn(2)–C(19) = 2.095(6) Å, Sn(2)–C(20) = 2.096(5) Å, Sn(2)–O(2) = 2.775(2) Å and Sn(2)–O(5′) = 2.040(2) Å (**1**), while in (**2**) they are as follows: Sn(2)–C(25) = 2.108(6) Å, Sn(2)–C(29) = 2.096(5) Å, Sn(2)–O(2) = 2.791(6) Å and Sn(2)–O(5′) = 2.040(2) Å. The mean values of the angles at the equatorial positions in (1) and (2), 93.3° and 92.7°, are a bit wider than the expected value, 90°.

Complexes (**3**) crystallizes in the monoclinic system with space group $P2_1/n$ ($Z = 2$). The staggered drum-like framework comprises the association of two six-member $(–Sn–O–)_3$ stannoxane rings, outlining the top and bottom faces of the drum, which are twisted by 60°. Its sides are shaped by six distorted square faces, described by bridging Sn–oxide interactions, joining together the neighbouring stannoxane hexamers. Each face is covered by bidentate valproate ligands, bridging diagonal tin atoms, and sustaining the integrity of the aggregate, assembling a mill wheel with zigzag blades, Figs. 6 and 7.

The asymmetric unit is formed by one stannoxane hexamers, $[SnPh\{OVp)_2\}O]_3$, comprising half of the molecule. Each half relates to the other by symmetry, in view of an inversion centre present in the centre of the drum. The Sn(IV) cations are chemically and magnetically equivalent and each of them are coordinated to three different groups: phenyl ring, valproate anion, and one oxygen (oxide). A pseudo octahedral geometry is observed at each Sn(IV) atoms, where one of the axial coordination is

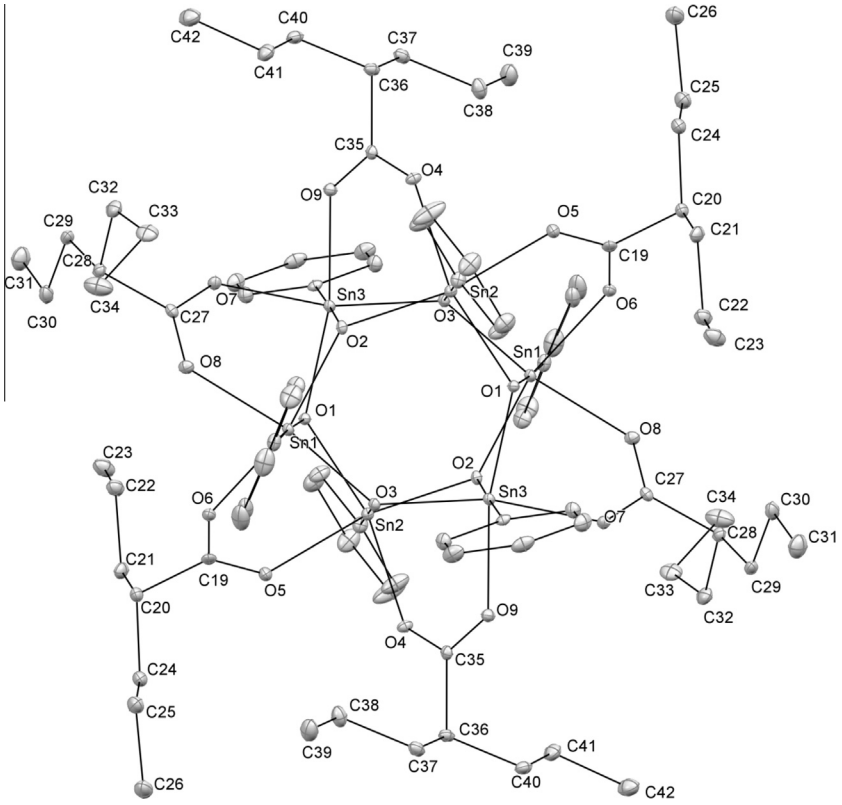

Fig. 6. The molecular structure of [{PhSn(O)OVp}$_6$] (**3**), view 1.

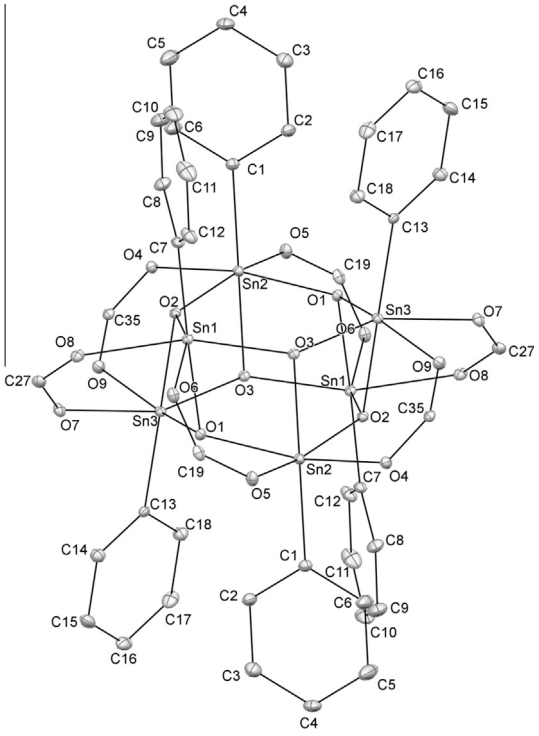

Fig. 7. The molecular structure of [{PhSn(O)OVp}$_6$] (**3**), view 2.

occupied by the Ph ring. The deformation arises from distorted angle and asymmetric bonding scheme. For instance, the Ph–Sn–O angle deviates from 180°, situating between 178.3(2)–179.3(1)° (oxygen trans to Ph). In addition the Ph–Sn–O angles (oxide cis to Ph), found in the range of 100.3(1)° to 103.0(1)°, are wider than those Ph–Sn–O angles (valproate oxygen cis to Ph), varying from 91.1(1)°–93.3(1)°. Finally, the four-member ring, composing the faces of the drum, are not planar but somewhat bent, with twisting angles ranging from 15.1(1)° to 15.8(1)°. The two alternated stannoxane rings (–Sn–O–)$_3$ adopt a double envelop chair-like conformation, with folding angles between 23.3 (3)° an 24.2 (2)°, Fig. 7. It is also observed in these rings the distance between the plans defined by the tin atoms, Sn (1′)–Sn(2)–Sn(3) and Sn(1)–Sn(2′)–Sn(3′), 2.3068 (4) Å is further apart in comparison with the separation of the plans shaped by the oxygen atoms, O(1)–O(2′)–O(3′) and O(1′)–O(2)–O(3′), 1.834 (4) Å. Despite the Sn(IV) cations are asymmetric coordinated by the O atoms, two different groups of Sn–O bonds are clearly observed in the structure. The bonds connecting the metal cations to the valproate ligand, in the range of 2.139 (3) Å and 2.164 (4) Å, are longer than the other Sn–O bonds, detected between 2.082 (3) and 2.100 (3) Å. It is also observed a symmetric coordination of the valproate group to the Sn(IV) cations in view of the small difference in the C–O bond lengths of the carboxylic moiety [1.260(5)–1.275(5) Å]. The 3D structure is held exclusively by van der Walls interactions of the valproate group and the peripheral phenyl ring. It might be a consequence of the steric hindrance of the structural arrangement preventing any intermolecular Sn–O association. Moreover, it is observed that the unit cells is formed by nine stannoxane rings, one in the centre and the remaining occupy the other corners, and each vertex is an inversion centre.

As observed in the literature organotin cage and cluster patterns can be displayed as hexagonal prismanes (drum-like structure), cubanes and ladders [43]. It has been demonstrated that the presence of other donor atoms, S, N or O in the ligand structure, can lead to other less common geometries [44].

4. Conclusions

Three new organotin valproates [{($Me_2SnOVp)_2O$}$_2$] (**1**), [{($Bu_2SnOVp)_2O$}$_2$] (**2**) and [{$PhSn(O)OVp$}$_6$] (**3**) have been obtained from the reaction of NaOVp with SnR_2Cl_2 {R = Me, Bu and Ph}. The compounds Me_2SnOVp_2 and Bu_2SnOVp_2 have been isolated and characterized as intermediates of (**1**) and (**2**). Their hydrolyses during the re-crystallization process produced the corresponding stannoxanes. The X-ray structures of the complexes revealed the rare coordination fashion of carboxylates towards organotin fragments with both bridging monodentate and bidentate ligand. The cleavage of a Sn–Ph bond in $SnPh_2Cl_2$, normally observed in strong acidic media, has occurred in the presence of NaOVp, producing complex (**3**). So, the coordination of valproate anions, oxide anions and organotin moiety in complex (**3**) led to the formation of a drum-like structure. The ^{119}Sn-NMR spectra in solution revealed the presence of major signals attributed the endo and exocyclic SnR_2 fragment in (**1**) and (**2**). On the other hand only the resonances of the endo and exocyclic organotins were detected in the solid state ^{119}Sn-NMR spectra of complex (**1**), however with quite different chemical shifts from those observed in solution. Therefore the structure of (**1**) in the solid state is not the same as in solution. The solid- and solution-state ^{119}Sn NMR experiments with complex (**3**) revealed only one signal with δ and δ_{iso} very close one to another.

Acknowledgements

This work was supported by CNPq, CAPES and FAPEMIG–Brazil.

Appendix A.

CCDC 1062377, 1062378 and 1062379; contains the supplementary crystallographic data of this paper. These data can be obtained free of charge via http://www.ccdc.cam.ac.uk/conts/retrieving.html, or from the Cambridge Crystallographic Data Centre, 12 Union Road, Cambridge CB2 1EZ, UK; fax: (+44) 1223-336-033; or e-mail: deposit@ccdc.cam.ac.uk.

References

[1] D. Liu, R.J. Maguire, Y.L. Lau, G.J. Pacepavicius, H. Okamaru, I. Aoyama, Water Res. 31 (1997) 2363.
[2] N. Voulvoulis, M.D. Scrimshaw, J.N. Lester, Appl. Organomet. Chem. 13 (1999) 135.
[3] R.J. Maguire, Water Qual. Res. J. Can. 26 (1991) 43.
[4] B. Chantong, D.V. Kratschmar, A. Lister, A. Odermatt, Toxicol Lett. 230 (2014) 177.
[5] K.E. Appel, Drug Metab. Rev. 36 (2004) 763.
[6] A.G. Davies, M. Gielen, K.H. Pannell, E.R.T. Tiekink, Tin Chemistry – Fundamentals, Frontiers and Applications, Wiley, Chichester, 2008.
[7] M. Sirajuddin, S. Ali, V. Mckee, M. Sohail, H. Pasha, Eur. J. Med. Chem. 84 (2014) 343.
[8] F. Arjmand, M. Muddassir, I. Yousuf, J. Photochem. Photobiol. B 136 (2014) 62.
[9] M. Yousefi, M. Safari, M.B. Torbati, A. Amanzadeh, J. Struct. Chem. 55 (2014) 101.
[10] H. Tlahuext, R. Reyes-Martinez, G. Vargas-Pineda, M. Lopez-Cardoso, H. Hopfl, J. Organomet. Chem. 696 (2011) 693.
[11] A. Husain, S.A.A. Nami, K.S. Siddiqi, J. Mol. Struct. 970 (2010) 117.
[12] J.P. Fuentes-Martinez, I. Toledo-Martinez, P. Roman-Bravo, P.G.Y. Garcia, C. Godoy-Alcantar, M. Lopez-Cardoso, H. Morales-Rojas, Polyhedron 28 (2009) 3953.
[13] A. Normah, K.N. Farahana, B. Ester, H. Asmah, N. Rajab, A.A. Halim, Res. J. Chem. Environ. 15 (2011) 544.
[14] R. Singh, N.K. Kaushik, Spectroc. Acta A 71 (2008) 669.
[15] E. Santacruz-Juarez, J. Cruz-Huerta, I.F. Hernandez-Ahuactzi, R. Reyes-Martinez, H. Tlahuext, H. Morales-Rojas, H. Hopfl, Inorg. Chem. 47 (2008) 9804.
[16] S. Shahzadi, S. Ali, M. Fettouhi, J. Chem. Crystallogr. 38 (2008) 273.
[17] G. Yenişehirli, N.A. Öztaş, E. Şahin, M. Çelebier, N. Ancın, S.G. Öztaş, Heteroat. Chem. 21 (2010) 373.
[18] T.S.B. Baul, Appl. Organomet. Chem. 22 (2008) 195.
[19] J.S. White, J.M. Tobin, J.J. Coney, Can. J. Microbiol. 45 (1999) 541.
[20] J.J. Cooney, S. Wuertz, J. Ind. Microbiol. 4 (1989) 375.
[21] J.J. Cooney, S. Wuertz, J. Indust. Microbiol. 4 (1989) 375.
[22] D.C. Menezes, G.M. de Lima, A.O. Porto, M.P. Ferreira, J.D. Ardisson, R.A. Silva, Main Group Met. Chem. 30 (2007) 49.
[23] D.C. Menezes, G.M. de Lima, G.S. de Oliveira, A.V. Boas, A.M.A. Nascimento, F.T. Vieira, Main Group Met. Chem. 31 (2008) 21.
[24] D.C. Menezes, F.T. Vieira, G.M. de Lima, J.L. Wardell, M.E. Cortes, M.P. Ferreira, M.A. Soares, A.V. Boas, Appl. Organomet. Chem. 22 (2008) 221.
[25] D.C. Menezes, G.M. de Lima, F.A. Carvalho, M.G. Coelho, A.O. Porto, R. Augusti, J. D. Ardisson, Appl. Organomet. Chem. 24 (2008) 650.
[26] A. Duenas-Gonzalez, M. Candelaria, C. Perez-Plascencia, E. Perez-Cardenas, E. de la Cruz-Hernandez, L.A. Herrera, Cancer Treat. Rev. 34 (2008) 206.
[27] O. Pellerito, C. Prinzivalli, E. Foresti, P. Sabatino, M. Abbate, G. Casella, T. Fiore, M. Scopelliti, C. Pellerito, M. Giuliano, G. Grasso, L. Pellerito, J. Inorg. Biochem. 16 (2013) 125.
[28] B.P. de Morais, G.M. de Lima, D.C. Menezes, R.A.S. San Gil, C.B. Pinheiro, J. Mol. Struct. 1094 (2015) 246.
[29] G.M. Sheldrick, Acta Crystallogr. A 64 (2008) 112.
[30] G.M. Sheldrick, SHELXL-97. Program for Crystal Structure Refinement, University of Göttingen, Germany, 1997.
[31] L.J. Farrugia, J. Appl. Crystallogr. 30 (1997) 565.
[32] C.F. Macrae, P.R. Edgington, P. McCabe, E. Pidcock, G.P. Shields, R. Taylor, M.J. van De Streek, J. Appl. Crystallogr. 39 (2006) 453.
[33] R.K. Ingham, Chem. Rev. 60 (1960) 459.
[34] J. Beckmann, M. Henn, K. Jurschat, M. Schürmann, Organometallics 21 (2002) 192.
[35] M. Nath, S. Pokharia, X. Song, G. Eng, M. Gielen, M. Kemmer, M. Biesemans, R. Willem, D. de Vos, Appl. Organomet. Chem. 17 (2003) 305.
[36] M.A. Abdellah, S.K. Hadjikakou, N. Hadjiliadis, M. Kubicki, T. Bakas, N. Kourkoumelis, Y.V. Simos, S. Karkabounas, M.M. Barsan, I.S. Butler, Bioinorg. Chem. Appl. (2009) 542979.
[37] B.P. Morais, G.M. de Lima, D.C. Menezes, C.B. Pinheiro, J.A. Takahashi, J.D. Ardisson, R.A.S.S. Gil, J. Mol. Struct. 1079 (2015) 246.
[38] G.B. Deacon, R.J. Phillips, Coord. Chem. Rev. 33 (1980) 227.
[39] A.G. Davies, H.J. Milledge, D.C. Puxley, P.J. Smith, J. Chem. Soc. A (1970) 2862.
[40] P.J. Smith, Organomet. Chem. Rev. A 5 (1970) 373.
[41] P.T. Greene, R.F. Bryan, J. Chem. Soc. A (1971) 2549.
[42] V. Chandrasekhar, K. Gopal, P. Sasikumar, R. Thirumoorthi, Coord. Chem. Rev. 249 (2005) 1745.
[43] C.L. Ma, S.L. Zhang, Z.S. Hu, R.F. Zhang, J. Coord. Chem. 65 (2012) 2569.
[44] J.H. Zhang, R.F. Zhang, C.L. Ma, D.Q. Wang, H.Z. Wang, Polyhedron 30 (2011) 624.